Myeloid-derived suppressor cells mediate tolerance induction in autoimmune disease

Short title: MDSCs mediate tolerance induction

Anja Wegner[1,2], Johan Verhagen[1,3], David C. Wraith[1,4]

1. University of Bristol, School of Cellular and Molecular Medicine, Biomedical Sciences Building, University Walk, Bristol, BS8 1TD
2. Current address: CAR Mechanics group, Research Oncology, King's College London, Guy's Hospital, Great Maze Pond, London, SE1 9RT
3. Current address: Peter Gorer Department of Immunobiology, King's College London, Guy's Hospital, Great Maze Pond, London, SE1 9RT
4. Current address: Institute of Immunology and Immunotherapy, College of Medical and Dental Sciences, University of Birmingham, Birmingham B15 2TT

Corresponding author: D.C. Wraith

Key words: Myeloid-derived suppressor cells, tolerance, autoimmune disease, immunotherapy, experimental autoimmune encephalomyelitis

Abbreviations: CNS; central nervous system, MS; Multiple Sclerosis, MDSC; myeloid-derived suppressor cell, polymorphonuclear MDSC; PMN-MDSC, monocytic MDSC; M-MDSC, MBP; myelin basic protein, EAE; experimental autoimmune encephalomyelitis, DC; dendritic cell, ILN; inguinal lymph node, BLN; brachial lymph node, IDO; indoleamine 2,3-dioxygenase, APC; antigen-presenting cell, EDI; escalating dose immunotherapy, AUC; area under the curve, Ag; antigen, s.c.; subcutaneous, i.p.; intraperitoneal, Tnaiv; naïve T cells, Tag; antigen-experienced T cells, Treg; regulatory T cells, CFA; complete Freund's adjuvant

Summary

In multiple sclerosis (MS) T cells aberrantly recognise self-peptides of the myelin sheath and attack the central nervous system (CNS). Antigen-specific peptide immunotherapy, which aims to restore tolerance while avoiding the use of non-specific immunosuppressive drugs, is a promising approach to combat autoimmune disease, but the cellular mechanisms behind successful therapy remain poorly understood. Myeloid-derived suppressor cells (MDSCs) have been studied intensively in the field of cancer and to a lesser extent in autoimmunity. Because of their suppressive effect on the immune system in cancer, we hypothesised that the development of MDSCs and their interaction with $CD4^+$ T cells could be beneficial for antigen-specific immunotherapy. Thus, changes in the quantity, phenotype and function of MDSCs during tolerance induction in our model of MS were evaluated. We reveal, for the first time, an involvement of a subset of MDSCs, known as polymorphonuclear (PMN)-MDSCs, in the process of tolerance induction. PMN-MDSCs were shown to adopt a more suppressive phenotype during peptide immunotherapy and inhibit $CD4^+$ T cell proliferation in a cell contact-dependent manner, mediated by arginase-1. Moreover, increased numbers of tolerogenic PMN-MDSCs, such as observed over the course of peptide immunotherapy, were demonstrated to provide protection from disease in a model of experimental autoimmune encephalomyelitis (EAE).

Introduction

Multiple sclerosis (MS) is a chronic inflammatory disorder of the central nervous system where immune cells attack myelinated axons of the brain and spinal cord (1). The ideal treatment of MS would be to specifically target the disease-causing immune cells without compromising the broader function of the immune system. A promising approach to the treatment of MS relies on the use of soluble, synthetic peptides, based on the sequence of known disease-associated antigens, to promote tolerance induction. In the Tg4 model of experimental autoimmune encephalomyelitis (EAE), T cells express a transgenic TCR specific for the immunodominant epitope of Myelin Basic Protein, MBPAc1-9 (2). The development of induced EAE in this model can be prevented by repetitive administration of the cognate peptide (3). This is characterised by the induction of anergy in $CD4^+$ T cells and a switch in serum cytokines from a dominant IFN-γ response towards IL-10. A dose escalation protocol for subcutaneous delivery of the high self-antigen doses, required for effective tolerance induction, was shown to be highly effective and safe (4, 5).

Escalating dose immunotherapy (EDI) leads to an upregulation of co-inhibitory molecules including LAG-3, TIGIT, TIM-3 and PD1 on $CD4^+$ T cells (5). Another study previously found that expression of TIM-3 on T cells resulted in the increase in a population of $CD11b^+$ $Ly6G^+$ cells (6). These innate cells, known as myeloid-derived suppressor cells (MDSCs), were first described more than 30 years ago in cancer patients (7). Since then, their detrimental role in cancer has been well characterised. These immature myeloid cells accumulate in tumours and contribute highly to immune escape by suppressing antigen-

specific T cell responses (8, 9). Only more recently has a potential beneficial role for MDSCs in autoimmune diseases, including Type-1 diabetes (10) and EAE (11) become appreciated, demonstrating that MDSCs can limit T cell-mediated pathology and tissue injury. In mice, MDSCs are broadly defined as $CD11b^{+}$ $Gr1^{+}$ cells. Anti-Gr1 antibodies recognise two targets, LY6G and LY6C. A further distinction in MDSC subsets can be made based on their differential LY6G and LY6C expression (12). Polymorphonuclear MDSCs (PMN-MDSCs) have a $CD11b^{+}$ $LY6G^{+}$ $LY6C^{low}$ phenotype, whereas MDSCs with monocytic morphology (M-MDSCs) are $CD11b^{+}$ $LY6G^{-}$ $LY6C^{hi}$ (13). MDSCs use multiple mechanisms to suppress T cell proliferation. The majority of studies have found an involvement of the enzymes arginase-1 and iNOS in MDSC-mediated suppression of T cells (14, 15). More recently, other mechanisms of suppression deployed by MDSCs have been revealed, including the production of the enzyme indoleamine 2,3-dioxygenase (IDO) and IL-10 (16, 17). In addition to these soluble factors, cell surface molecules, including PD-L1, Galectin-9, CD40 and CD80, have been suggested to play a role in the suppression of T cells, (6, 18-20). Here, we reveal for the first time a previously unknown role for PMN-MDSCs in antigen-specific tolerance induction.

Materials and Methods

Mice

All animal experiments were carried out under a UK Home Office Project Licence and approved by the University of Bristol ethical review committee. Mice were bred and kept under specific pathogen-free conditions.

The Tg4 T cell receptor (TCR)-transgenic mouse was described previously (21). $CD4^+$ T cells in this model express a Vα4 Vβ8.2 transgenic TCR specific for the acetylated nine-residue peptide of MBP (Ac1-9) in the context of I-Au.

Peptides

MBP_{Ac1-9}(4K) (Ac-ASQKRPSQR) and the high affinity analogue MBP_{Ac1-9}(4Y) (Ac-ASQYRPSQR) were custom-synthesized by GL Biochem Shanghai.

Escalating-dose peptide immunotherapy

For tolerance induction, mice were treated subcutaneous (s.c.) every 3–4 days with a total of 6 doses of MBP_{Ac1-9}(4Y) in PBS in increasing doses: 0.08μg, 0.8μg, 8μg, 3 x 80μg.

Flow cytometry analysis

The following anti-mouse antibodies (Biolegend unless stated otherwise) were used: CD4 A700, IL-17A PerCP-Cy5.5 (eBioscience), IFN-γ APC (eBioscience), Foxp3 PE (eBioscience), Ly6G A700, Ly6C APC-Cy7, CD11b PerCP-Cy5.5, Galectin-9 PE, CD80 BV421, CD86 BV605, CD40 PE-Cy7, PD-L1 APC, MHCII APC-Cy7. Fixable viability dye-eFluor780 (eBioscience) was used to exclude

dead cells. Samples for intracellular staining were activated with 5 ng/ml PMA (Sigma) plus 500ng/ml Ionomycin (Sigma) and Golgi Stop (BD Bioscience) for three hours. Cell proliferation dye-ef450 (CPD-ef450, eBioscience) was used to visualize cell divisions or calculate division and proliferation indexes. FACS acquisition was performed on an LSR-II flow cytometer (Becton-Dickinson) and results were analysed using FlowJo software (TreeStar Inc).

Magnetic cell isolation

Naïve $CD4^+$ T cells were isolated using the MagniSort™ Mouse CD4 Naïve T cell Enrichment Kit (#8804-6824-74) from eBioscience according to the instructions. Mouse $CD11c^+$ dendritic cells (DCs) from the spleen were isolated using the CD11c Microbeads Kit from MACS Miltenyi (#130-052-001).

^{3}[H]-Thymidine proliferation assay

For some ^{3}[H]-thymidine proliferation assays, $1x10^6$ splenocytes or $2x10^5$ lymph node cells were cultured, in triplicate, with titrated doses of MBP_{Ac1-9}(4K) in a 96-well round bottom plate. For other experiments, $CD4^+$ T cells were magnetically isolated from the spleen and a ^{3}[H]-Thymidine assay was set up with titrated doses of MBP_{Ac1-9}(4K) and irradiated APCs. Cells were cultured for three days at 37°C in a CO_2 incubator and 0.5 μCi of ^{3}[H]-Thymidine was added to wells for 16 h before measurement using a 1450 Micro-β counter (Wallac).

***In vitro* suppression assay**

PMN-MDSC and antigen-experienced $CD4^+$ T cells (Tag) from MBP_{Ac1-9}(4Y)-treated mice were FACS sorted. PMN-MDSCs and $CD4^+$ T cells were either co-

cultured at a ratio of 1:3 together with $CD11c^+$ cells as antigen-presenting cell (APC) in a APC:T cell ratio of 1:10 and MBP_{Ac1-9}(4K)-peptide (10μg/ml) or at a 1:1 ratio in the presence of 1 μg/ml plate-bound anti-CD3 and 2 μg/ml anti-CD28 (both from BioXCell). Both $CD4^+$ T cell populations were labelled with cell proliferation dye eFluor®450 before co-culture. $1x10^6$ $CD4^+$ T cells were used for the co-culture for four days in a 48-well plate or $1x10^5$ T cells in a 96-well plate. Some experiments were performed in the presence of neutralising antibodies against: PD-L1, Galectin-9, CD40, CD80, CD86 (all from Biolegend) and IL-10R (BioXCell). For experiments regarding the effect of iNOS and arginase-1, 0.5 mM L-NMMA (Merck) or 0.5 mM BEC (Santa Cruz Biotechnology) respectively were added at the beginning of the culture. To investigate if the suppressive effect of PMN-MDSC is contact dependent, PMN-MDSC and $CD4^+$ T cells were separated during the co-culture using a transwell assay (Corning).

Induction and evaluation of EAE

EAE was induced by adoptive transfer of MBP_{Ac1-9}-specific Th1 cells. Briefly, Tg4 splenocytes were cultured for 5 days with 10 μg/ml MBP_{Ac1-9}(4K) and 5 ng/ml rmIL-12 (PeproTech), in the presence or absence of PMN-MDSCs from tolerised Tg4 mice at a ratio of 1:3. 20 U/ml rhIL-2 (R&D Systems) was added after 72 h. *In vitro*-polarized Th1 cells ($5×10^6$) were transferred into Tg4 animals. EAE was assessed twice daily with the following scoring system: 0, no signs; 1, flaccid tail; 2; impaired righting reflex and/or gait; 3, hind limb paralysis; 4, forelimb and hind limb paralysis; 5, moribund.

Results

Increase in M-MDSCs and PMN-MDSCs during EDI

Two subpopulations of MDSCs are currently defined in mice; monocytic MDSCs (M-MDSCs) characterised by a $CD11b^{+}$ $Ly6G^{-}$ $Ly6C^{high}$ phenotype and polymorphonuclear MDSCs (PMN-MDSCs) that have a $CD11b^{+}$ $Ly6G^{+}$ $Ly6C^{low}$ phenotype. We observed that after a course of EDI with $MBP_{Ac1\text{-}9}$(4Y) the percentage of MDSCs among $CD11b^{+}$ cells had increased systemically compared to control-treated animals (Figure 1A). In the spleen, inguinal lymph nodes (ILN), brachial lymph nodes (BLN), liver, lung, brain and spinal cord, the increase in the percentage of PMN-MDSCs was more pronounced than that of M-MDSCs. The lung was the only organ where we observed an increase in the frequency of both MDSC subsets. Considering these results, we decided to concentrate on PMN-MDSCs for further experiments in which we assessed kinetics of MDSC changes during EDI. Expressed as a percentage of all leukocytes, the frequency of PMN-MDSCs peaked after the 3rd treatment in most organs other than the liver, where a significant increase was not established until the 5th treatment (Figure 1B). These experiments did not detect a statistically significant difference in the frequency of PMN-MDSCs in the spinal cord. In addition to the frequency of PMN-MDSCs, we also assessed absolute cell numbers for each organ (Figure 1C). These revealed a very similar pattern to the changes in the percentages.

Dose escalation immunotherapy alters PMN-MDSC phenotype

The pronounced accumulation of PMN-MDSCs after the 3rd dose of peptide treatment led us to further investigate PMN-MDSC phenotype and function at this point. At this time, $CD4^+$ T cells also start to undergo phenotypic changes that characterise the EDI protocol, namely the reduction in effector cytokines and the switch to IL-10-production in $CD4^+$ T cells (5). To further characterise the phenotype of PMN-MDSCs and find ways in which they might influence the function of $CD4^+$ T cells during the course of EDI, we investigated several markers that can affect $CD4^+$ T cell activation, including Galectin-9, PD-L1, CD40, CD80 and CD86. Representative staining of splenic PMN-MDSCs is shown in Figure 2A. The extent to which expression of these markers on PMN-MDSCs was altered by EDI varied greatly depending on the location of the cells. For example, Galectin-9, PD-L1 and CD86 expression was increased on splenic PMN-MDSC compared to mice receiving PBS only as a control (Figure 2B). In other organs, such as the lung, Galectin-9 was increased but PD-L1 decreased in comparison to control-treated animals. There was no difference in CD40 expression in any of the organs evaluated. CD80 expression on PMN-MDSCs trended towards a reduction in $MBP_{Ac1\text{-}9}$(4Y)-treated animals but this was significant only in the ILNs.

Splenic PMN-MDSC suppress antigen-mediated proliferation of naïve $CD4^+$ T cells *in vitro*

In order to establish whether the PMN-MDSCs that developed during EDI do indeed have immune regulatory properties, we first assessed their effect on

$CD4^+$ T cell proliferation *in vitro*. Naïve Tg4 $CD4^+$ T cells (Tnaiv) and antigen-experienced $CD4^+$ T cells (Tag) labelled with cell proliferation dye were co-cultured with $CD11c^+$ APCs and 10 μg/ml of cognate peptide, in the presence or absence of PMN-MDSCs from tolerised mice. After the four-day co-culture we measured $CD4^+$ T cell proliferation by flow cytometry and calculated the proliferation and division indexes. These experiments revealed that addition of PMN-MDSCs to the T cell cultures reduced the division index of proliferating naïve $CD4^+$ T cell, but to our surprise, PMN-MDSCs were unable to reduce the proliferation of $CD4^+$ Tag cells (Figure 3A). Importantly, addition of PMN-MDSCs led to the expansion of $CD4^+$ $Foxp3^+$ regulatory T cells within the $CD4^+$ T cell population, although this only reached statistical significance for the combined data from 5 separate co-cultures with $CD4^+$ Tag cells (Figure 3B). This could potentially be explained by the additional requirement of IL-2 for optimal $CD4^+$ Treg cell expansion. This cytokine is secreted abundantly by $CD4^+$ Tag cells but not naïve $CD4^+$ T cells.

Splenic PMN-MDSC suppress the proliferation of antigen-experienced $CD4^+$ T cells activated by a polyclonal stimulus *in vitro* in a cell-contact dependent manner

Next we sought to determine if, in addition to suppression of an antigen-driven response, PMN-MDSC in the Tg4 model could act as suppressors of $CD4^+$ T cell proliferation activated *in vitro* without antigen or APC. Either Tnaiv or Tag cells, labelled with proliferation dye, were cultured together with PMN-MDSCs from tolerised mice at a ratio of 1:1 for four days on a plate coated with anti-CD3 and anti-CD28. The suppressive activity of PMN-MDSCs is their main

characteristic but to make sure that this suppressive ability is the result of tolerance induction through EDI, we also isolated PMN-MDSCs from PBS-treated mice as a control and included those in our proliferation assays. PMN-MDSCs from tolerised mice were found to be potent suppressors because they reduced the division index of both naïve $CD4^+$ T cells and antigen-experienced T cells significantly (Figure 4A+B). On the other hand, PMN-MDSCs from control mice were not able to reduce the proliferation. In order to determine if the suppressive activity seen before is cell contact-dependent, transwell experiments were performed. In these experiments, $CD4^+$ Tag cells were cultured on an anti-CD3+anti-CD28-coated plate, separated by a membrane from splenic, FACS-sorted PMN-MDSC from tolerised Tg4 mice. Physical separation of PMN-MDSCs and responder cells abrogated the suppressive effect on $CD4^+$ T cell proliferation, which suggested that the PMN-MDSC-mediated suppression of $CD4^+$ T cell proliferation is cell contact-dependent (Figure 3C).

PMN-MDSCs use a range of suppressive mechanisms

Several molecules have previously been suggested to mediate cell contact-dependent suppression by PMN-MDSCs. To investigate the molecules that may be involved in the suppressive effect of PMN-MDSCs, blocking antibodies targeting molecules expressed on the surface of PMN-MDSCs, namely Galectin-9, PD-L1, CD40, CD80 and CD86, or anti-IL-10R were added to the co-culture. The suppressive activity of PMN-MDSCs was impaired under several of these conditions (Figure 5A). The addition of either anti-Galectin-9 or PD-L1 alone did not abrogate the suppressive activity of PMN-MDSCs whereas

the co-blockade of both ligands restored $CD4^+$ T cell proliferation at least in part, indicating a synergistic effect of Galectin-9 and PD-L1 in $CD4^+$ T cell suppression. The addition of blocking antibodies targeting the surface molecules CD40, CD80 or CD86 restored $CD4^+$ T cell proliferation in a similar fashion. IL-10 receptor signalling, however, did not appear to be essential for the suppressive activity of PMN-MDSCs because in our *in vitro* suppression assay blockade of IL-10R (Figure 5A) did not alleviate $CD4^+$ T cell suppression. In addition to these cell surface antigens, soluble factors may still be involved in mediating suppression of $CD4^+$ T cells in close proximity. Therefore, the possible role of iNOS and arginase-1 in mediating the suppression of $CD4^+$ T cell proliferation was investigated further by the addition of an inhibitor of iNOS, (NG-monomethyl-L-arginine (L-NMMA), or an inhibitor of arginase-1, (S-(2-boronoethyl)-L-cysteine (BEC) to the suppression assay (Figure 5B). The addition of the arginase-1 inhibitor but not iNOS inhibitor abrogated the suppressive effect of PMN-MDSCs.

Frequencies and phenotype of PMN-MDSCs in peripheral organs in diseased versus tolerised mice

The role of MDSCs in autoimmunity remains controversial. On the one hand, the accumulation of $CD11b^+Ly6C^{high}$ M-MDSCs in EAE positively correlated with disease severity and an improvement in pathology was accompanied by the reduction of these cells (22, 23). However, in contrast to these studies their beneficial role in autoimmune diseases including EAE has become increasingly appreciated in recent years (11). MDSCs have been shown to be able to limit T cell-mediated pathology and tissue injury as a result of their suppressive activity

(24). To assess the dynamics of PMN-MDSCs during EAE in the TG4 model, mice were treated with MBP_{Ac1-9}(4Y) to confer protection or with PBS only as a control, prior to the induction of EAE. Animals were culled at the peak of disease when PBS-treated animals had an average disease score of 3 with complete hind limb paralysis (typically around day 14 post immunisation). MBP_{Ac1-9}(4Y)-treated animals, which displayed no EAE symptoms, were taken at the same time of analysis. This confirmed that the frequency of PMN-MDSCs was increased in animals in which EAE was induced compared to animals that were not primed for disease (Figure 6A compared to Figure 1B). In fact, the frequency of PMN-MDSC in mice with EAE was significantly higher in many of the organs examined than in mice that had been tolerised using EDI (Figure 6A). This then prompted the question whether qualitative changes may be more important for the immunosuppressive of MDSCs than quantitative changes. We therefore examined if the PMN-MDSC that arise during the development of EAE are phenotypically different from the ones that are generated during tolerisation. Indeed, we observed a significant two-fold lower expression of CD40 on PMN-MDSCs in the spinal cord of mice with EAE compared to tolerised animals (Figure 6B). Furthermore, we detected a significantly lower expression of CD80 in the CNS compartment both in the brain and spinal cord, in tolerised animals compared to animals with EAE (Figure 6B). Finally, we found an increased expression of Galectin-9 and PD-L1 in both the spleen and lymph nodes in tolerised mice compared to control mice. However, the expression levels of these two markers in tolerised animals differ greatly between the spleen and inguinal lymph nodes in particular (Figure 6B). These findings hint at the

possibility that phenotypic differences between the PMN-MDSCs that develop after EAE development or after tolerisation play a role in their functional dichotomy.

Splenectomy impairs the increase in the number of PMN-MDSCs post EDI and prevents tolerance induction

We demonstrated an increase in the number of splenic PMN-MDSCs, with a marker profile distinct from PMN-MDSCs residing in the lymph nodes. Therefore, we wanted to further investigate the role of the spleen in tolerance induction. To achieve this, we performed splenectomies or sham operations prior to tolerance induction in Tg4 mice and analysis of the number of PMN-MDSCs in the lymph nodes, lung or liver. As shown in Figure 7A+B, splenectomy resulted in a statistically significant abrogation of the increase in the percentage of PMN-MDSCs after EDI only in the ILNs, although a similar trend was observed in the BLNs and, in particular, the liver. Furthermore, we found that an intact spleen was essential for successful tolerance induction with $MBP_{Ac1\text{-}9}$(4Y). Removal of the spleen did not affect disease development in control-treated animals (Figure 7C), whereas animals receiving $MBP_{Ac1\text{-}9}$(4Y)-treatment after a sham operation were largely protected against the induction of EAE. Their splenectomised counterparts all developed severe EAE. In order to allow for statistical analysis of the EAE scores of all animals over the course of the experiment, the area under the curve (AUC) was calculated and this demonstrated the same trend (Figure 7C).

Signalling through the IL-10 receptor controls PMN-MDSC accumulation and phenotype

Our previous data showed that IL-10 receptor signalling is not essential for the suppressive activity of PMN-MDSCs because blockade of IL-10R signalling by an antibody did not alleviate $CD4^+$ T cell suppression *in vitro* (Figure 5A). However, we were still interested to know if IL-10 signalling affects the quantity and phenotype of PMN-MDSCs. First, we treated Tg4IL-$10^{-/-}$ mice with either PBS or MBP_{Ac1-9}(4Y) according to the EDI protocol until the 3rd dose before isolating the spleen and lymph nodes to determine the quantity of PMN-MDSCs. The significant increase of PMN-MDSCs that results from peptide treatment in IL-10-sufficient animals was impaired in spleen and lymph nodes of Tg4IL-$10^{-/-}$ mice (Figure 8A+B). This was true for both the increase in the percentage and absolute number of PMN-MDSCs in the lymph nodes (Figure 8A+B). The fact that we detected fewer PMN-MDSCs in IL-$10^{-/-}$ animals could be either a direct effect because MDSCs can express IL-10R (25) or an indirect effect of excess $CD4^+$ T cell activation in response to antigenic challenge in IL-$10^{-/-}$ mice. The reduction in the number of PMN-MDSCs in Tg4IL-$10^{-/-}$ animals led us to further characterise the phenotype of PMN-MDSC in this model. The reduction of CD80 expression commonly observed in wild-typeTg4 mice after MBP_{Ac1-9}(4Y)-treatment is abrogated in IL-$10^{-/-}$ mice (only statistically significant in the ILNs) (Figure 8C). Moreover, the substantial increase of CD86 expression on PMN-MDSCs from wild-type Tg4 mice in the spleen post EDI was impaired in Tg4IL-$10^{-/-}$ mice (Figure 8D).

PMN-MDSCs reduce CD4$^+$ T cell proliferation after antigen challenge *in vivo*

In order to test if, in addition to their inhibitory effect *in vitro*, PMN-MDSCs are able to reduce the proliferation of CD4$^+$ T cells *in vivo*, Tg4 mice received a cell transfer of 1.5x10^6 FACS-sorted PMN-MDSC from tolerised mice i.p. three days before priming with MBP$_{Ac1-9}$(4K) peptide in complete Freund's adjuvant (CFA) at the base of the tail. Ten days later, spleen and ILNs were harvested and a ^{3}[H]-Thymidine assay was set up. The proliferative response after restimulation *in vitro* with cognate peptide was significantly reduced in cells from the spleen but not the ILNs from mice that had received a transfer of PMN-MDSCs compared to mice that did not receive PMN-MDSCs (Figure 9A). Next, to exclude the possibility that transferred PMN-MDSCs still present in the whole splenocyte suspensions mediate suppression of CD4$^+$ T cell proliferation at the time of restimulation *in vitro*, CD4$^+$ T cells were magnetically isolated from the spleen and a separate ^{3}[H]-Thymidine assay was set up with titrated doses of MBP$_{Ac1-9}$(4K) and irradiated APCs. Again, the proliferation of CD4$^+$ T cells isolated from mice that had received a transfer of PMN-MDSCs was significantly reduced over a range of MBP$_{Ac1-9}$(4K) peptide concentration compared to cells from mice that did not receive the transfer (Figure 9B). In addition, intracellular cytokine staining demonstrated a small but not significant reduction in the production of the proinflammatory cytokines IFN-γ or IL-17 by CD4$^+$ T cells from animals that had received a PMN-MDSC transfer, upon restimulation with PMA/Ionomycin (Figure 9C).

PMN-MDSCs ameliorate encephalogenicity of Th1 cells.

Given the reduction in $CD4^+$ T cell proliferative capacity after adoptive transfer of PMN-MDSCs *ex vivo*, we asked if PMN-MDSCs would interfere with $CD4^+$ T cell pathogenicity. Therefore, MBP-specific $CD4^+$ T cells were polarised *in vitro* under normal Th1 conditions either with or without the addition of PMN-MDSCs, prior to adoptive transfer to Tg4 recipients to induce a passive form of EAE. The addition of PMN-MDSC during Th1 polarisation led to a clear amelioration of EAE severity and to an enhanced recovery from disease, demonstrating their disease-limiting propensity (Figure 10 and Table 1).

Discussion

In this study, we show for the first time that MDSCs, and PMN-MDSCs in particular, accumulate during the course of EDI in various organs from the CNS to the periphery. The preferential expansion of PMN-MDSCs over M-MDSCs does not come as a complete surprise because PMN-MDSCs represent the major pool of circulating and expanding MDSCs in both mice and humans in the tumour environment (26), revealing a 3:1 ratio of PMN-MDSCs to M-MDSCs (27). The more pronounced accumulation of PMN-MDSC after the 3rd dose of peptide treatment may result from the fact that Tg4 mice showed a peak in the amount of IL-6 and IL-17 after this dose (5). These cytokines are known to mediate the accumulation of MDSCs and their immunosuppressive function (28-31). The PMN-MDSCs that we induced during antigen-specific peptide immunotherapy were able to reduce the proliferation of CD4$^+$ T cells and expand CD4$^+$ Foxp3$^+$ T cells *in vitro*. Moreover, adoptive transfer of PMN-MDSCs prior to priming of Tg4 mice with MBP$_{Ac1\text{-}9}$(4K) in CFA reduced the CD4$^+$ T cell proliferative response upon restimulation *ex vivo*. We found that PMN-MDSCs were able to suppress naïve CD4$^+$ T cell proliferation induced by either an antigen-specific or non-specific stimulus. Surprisingly, PMN-MDSCs reduced the proliferative response of antigen-experienced T cells only when stimulated non-specifically with anti-CD3+anti-CD28. A previous study showed that MDSCs from the tumour site and spleen of the same mouse can differ in their ability to suppress CD8$^+$ T cell proliferation even though no phenotypic differences could be detected(31). Both MDSC-populations were able to suppress CD8$^+$ T cell proliferation in an antigen-specific manner, however

splenic MDSCs did not suppress $CD8^+$ T cell proliferation in response to anti-CD3+anti-CD28. These differences in suppression could be explained by the tumour environment, where suppressive factors are present that are absent in the spleen. But, all PMN-MDSCs we studied were isolated from the spleen and only the method of $CD4^+$ T cell stimulation differed. So far, we have no definitive explanation as to why in our experiments antigen-experienced cells could be suppressed when stimulated with antibody but not when stimulated with antigen, but it could have to do with either the affinity of the interaction or the involvement of co-stimulatory or co-inhibitory molecules. It further remains to be determined if the fact that the antigen-experienced T cells in our experiments have had more than one previous antigen encounter affects their ability to be suppressed by MDSCs.

Most of the published studies, as well as our own results, indicate that MDSCs need direct cell-cell contact to exert their immunosuppressive function, which suggests that they act either through cell surface receptor-ligand interactions or through release of soluble mediators that act only in close proximity (32). MDSCs have previously been shown to use multiple mechanisms to suppress T cell proliferation (14). The majority of studies have found an involvement of the enzymes arginase-1 and iNOS in MDSC-mediated suppression of T cells (14, 15). However, the addition of an inhibitor of iNOS, NG-monomethyl-L-arginine (L-NMMA) did not ablate the suppressive activity of PMN-MDSCs in our hands, whereas the arginase-1 inhibitor (BEC) restored $CD4^+$ T cell proliferation, thus suggesting a preferential role for arginase-1 in our model.

It has been suggested that the suppressive activity of MDSCs is dependent on the immunomodulatory cytokine IL-10 (17) although this finding is not universally supported (33). However, signalling through the IL-10-receptor was found to be required to establish the suppressive phenotype in MDSCs (33), which supports our findings that although addition of a blocking anti-IL-10R antibody did not restore $CD4^+$ T cell proliferation, tolerisation of IL-10-deficient animals showed a change in the phenotype of PMN-MDSCs compared to IL-10-sufficient mice.

In addition to these soluble factors, the cell surface molecules PD-L1 and Galectin-9 have been suggested to mediate the T cell suppressive effect (6, 18). In our study the blockade of either cell surface receptor separately during *in vitro* co-culture using neutralising antibodies did not restore T cell proliferation whereas the co-blockade of both molecules together led to the abrogation of suppression, indicating a synergistic effect.

The frequency of PMN-MDSC in mice with induced EAE was significantly higher in many of the organs examined than in mice that had been protected by EDI. This raises the question why animals are not protected from disease even though these potentially immunosuppressive PMN-MDSCs arise. Our findings hint at the possibility that phenotypic differences between those PMN-MDSCs that develop after EAE development and those that arise after tolerisation contribute to their functional dichotomy. Compared to the PMN-MDSCs of mice with EAE, we detected a higher expression of Galectin-9 and PD-L1 on PMN-MDSCs in the spleen and lymph nodes with an increase of CD40 and a decrease of CD80 in the CNS compartment of tolerised animals. The exact role

of CD40 in MDSC-mediated suppression remains unclear but Pan et al. showed that CD40 expressed on MDSCs is essential for their suppressive function and T reg cell induction (19). This is supported by our *in vitro* findings, where blockade of CD40 abrogated PMN-MDSC-suppression and restored $CD4^+$ T cell proliferation.

In recent years, the expression of CD80 on MDSCs has been associated with immune suppression (20), which corroborates our findings that the addition of anti-CD80 to our *in vitro* co-cultures led to abrogation of MDSC-mediated inhibition of $CD4^+$ T cell proliferation. This, however, is in direct contrast to our hypothesis that peptide treatment promotes a more suppressive PMN-MDSC phenotype in the CNS, as we found a reduced expression of CD80 on PMN-MDSCs in the CNS of tolerised animals. The effect of CD80 expression on the function of PMN-MDSCs remains unclear however, as it was shown previously that, in a rat model of kidney allograft tolerance, blood-derived CD80-positive MDSCs have the same suppressive capacity as their CD80-negative counterparts (34). Overall, it is unclear how important the phenotype of PMN-MDSCs in the CNS is for the prevention of EAE as the maintenance of tolerance and prevention of disease development may very well be controlled in the periphery rather than the CNS. After all, removal of the spleen prevented successful tolerance induction and hence protection from disease. This was also shown previously in a model of experimental autoimmune uveoretinitis (EAU) where splenectomy likewise abrogated the induction of tolerance (35).

PD-L1 expression on PMN-MDSCs was increased only in the spleen and no other organs of tolerised animals. $PD\text{-}L1^+$ PMN-MDSCs could potentially

interact with PD-1-expressing $CD4^+$ T cells in the spleen (5). Tumour-infiltrating MDSCs from tumour-bearing mice have previously been shown to express high levels of PD-L1 and to be able to suppress the proliferation of $CD8^+$ T cells (18). MDSC-mediated T cell suppression may thus be mediated by the PD-L1-PD-1 axis and that this interaction is likely take to place in the spleen. Another important negative regulator of T cell activity, TIM-3, was significantly upregulated on $CD4^+$ T cells in the spleen of tolerised animals that were protected from EAE in our study (5). An earlier study described a potential role for the Tim-3/Galectin-9 pathway in MDSC proliferation (6).

Our results suggest that MDSC-mediated plasticity of conventional T cells in the spleen, and not just the differentiation of Treg cells might, at least in part, be responsible for the protective effect of EDI. After all, our splenectomy experiments showed that animals without a spleen receiving EDI were still more susceptible to EAE than mice that retained their spleen. Our findings are supported by a study where splenectomy prior to tolerance induction to OVA did not affect the number of $CD4^+$ Treg cells yet the establishment of skin tolerance could not be achieved (36). Previous work implied that T cells need to migrate through the spleen to become encephalitogenic and cause disease, in a process known as T cell licensing (37). One could speculate that PMN-MDSCs in the spleen may prevent T cell licensing, although this will require further investigation.

Our work further provides evidence for a direct effect of PMN-MDSCs on the encephalogenicity of Th1 cells, as T cells cultured in the presence of PMN-MDSCs are less potent inducers of EAE. Animals developed less severe EAE

symptoms and recovered faster from disease compared to animals that received Th1 cells polarised under normal conditions.

Overall, we demonstrate here that PMN-MDSCs play an important role in tolerance induction during antigen-specific immunotherapy of autoimmune disease. Their differentiation should therefore be a prime target of treatment and may be an indicator of successful therapy.

Acknowledgements

This work was funded through a Marie Curie Fellowship (ITN NeuroKine; 316722) provided by the European Union in partnership with Apitope. The authors would like to thank Dr Andrew Herman of the UoB FMVS Flow Cytometry Facility for advice and assistance and the staff of the UoB ASU for assistance with the breeding and maintenance of animals.

AW conceived the study, designed and performed experiments, analysed data and wrote the manuscript. JV helped to design experiments and co-wrote the manuscript. DCW critically edited the manuscript and supervised the study.

Conflict of Interest

The authors declare no competing financial interests.

1. Noseworthy JH, Lucchinetti C, Rodriguez M, & Weinshenker BG (2000) Multiple sclerosis. *The New England journal of medicine* 343(13):938-952.
2. Fairchild PJ, Wildgoose R, Atherton E, Webb S, & Wraith DC (1993) An autoantigenic T cell epitope forms unstable complexes with class II MHC: a novel route for escape from tolerance induction. *Int Immunol* 5(9):1151-1158.
3. Gabrysova L*, et al.* (2009) Negative feedback control of the autoimmune response through antigen-induced differentiation of IL-10-secreting Th1 cells. *The Journal of experimental medicine* 206(8):1755-1767.
4. Sabatos-Peyton CA, Verhagen J, & Wraith DC (2010) Antigen-specific immunotherapy of autoimmune and allergic diseases. *Current opinion in immunology* 22(5):609-615.
5. Burton BR*, et al.* (2014) Sequential transcriptional changes dictate safe and effective antigen-specific immunotherapy. *Nat Commun* 5:4741.
6. Dardalhon V*, et al.* (2010) Tim-3/galectin-9 pathway: regulation of Th1 immunity through promotion of CD11b+Ly-6G+ myeloid cells. *J Immunol* 185(3):1383-1392.
7. Buessow SC, Paul RD, & Lopez DM (1984) Influence of mammary tumor progression on phenotype and function of spleen and in situ lymphocytes in mice. *Journal of the National Cancer Institute* 73(1):249-255.
8. Almand B*, et al.* (2001) Increased production of immature myeloid cells in cancer patients: a mechanism of immunosuppression in cancer. *Journal of immunology* 166(1):678-689.
9. Kusmartsev S & Gabrilovich DI (2006) Role of immature myeloid cells in mechanisms of immune evasion in cancer. *Cancer immunology, immunotherapy : CII* 55(3):237-245.
10. Yin B*, et al.* (2010) Myeloid-derived suppressor cells prevent type 1 diabetes in murine models. *Journal of immunology* 185(10):5828-5834.

11. Zhu B*, et al.* (2007) CD11b+Ly-6C(hi) suppressive monocytes in experimental autoimmune encephalomyelitis. *J Immunol* 179(8):5228-5237.

12. Youn JI, Nagaraj S, Collazo M, & Gabrilovich DI (2008) Subsets of myeloid-derived suppressor cells in tumor-bearing mice. *Journal of immunology* 181(8):5791-5802.

13. Bronte V*, et al.* (2016) Recommendations for myeloid-derived suppressor cell nomenclature and characterization standards. *Nature communications* 7:12150.

14. Bronte V & Zanovello P (2005) Regulation of immune responses by L-arginine metabolism. *Nat Rev Immunol* 5(8):641-654.

15. Rodriguez PC & Ochoa AC (2008) Arginine regulation by myeloid derived suppressor cells and tolerance in cancer: mechanisms and therapeutic perspectives. *Immunol Rev* 222:180-191.

16. Yu J*, et al.* (2013) Myeloid-derived suppressor cells suppress antitumor immune responses through IDO expression and correlate with lymph node metastasis in patients with breast cancer. *J Immunol* 190(7):3783-3797.

17. Huang B*, et al.* (2006) Gr-1+CD115+ immature myeloid suppressor cells mediate the development of tumor-induced T regulatory cells and T-cell anergy in tumor-bearing host. *Cancer Res* 66(2):1123-1131.

18. Deng L*, et al.* (2014) Irradiation and anti-PD-L1 treatment synergistically promote antitumor immunity in mice. *J Clin Invest* 124(2):687-695.

19. Pan PY*, et al.* (2010) Immune stimulatory receptor CD40 is required for T-cell suppression and T regulatory cell activation mediated by myeloid-derived suppressor cells in cancer. *Cancer Res* 70(1):99-108.

20. Yang R*, et al.* (2006) CD80 in immune suppression by mouse ovarian carcinoma-associated Gr-1+CD11b+ myeloid cells. *Cancer Res* 66(13):6807-6815.

21. Liu GY*, et al.* (1995) Low avidity recognition of self-antigen by T cells permits escape from central tolerance. *Immunity* 3(4):407-415.

22. Mildner A*, et al.* (2009) CCR2+Ly-6Chi monocytes are crucial for the effector phase of autoimmunity in the central nervous system. *Brain* 132(Pt 9):2487-2500.

23. Yi H, Guo C, Yu X, Zuo D, & Wang XY (2012) Mouse CD11b+Gr-1+ myeloid cells can promote Th17 cell differentiation and experimental autoimmune encephalomyelitis. *J Immunol* 189(9):4295-4304.

24. Ioannou M*, et al.* (2012) Crucial role of granulocytic myeloid-derived suppressor cells in the regulation of central nervous system autoimmune disease. *J Immunol* 188(3):1136-1146.

25. Liu G*, et al.* (2014) SIRT1 limits the function and fate of myeloid-derived suppressor cells in tumors by orchestrating HIF-1alpha-dependent glycolysis. *Cancer Res* 74(3):727-737.

26. Dolcetti L*, et al.* (2010) Hierarchy of immunosuppressive strength among myeloid-derived suppressor cell subsets is determined by GM-CSF. *Eur J Immunol* 40(1):22-35.

27. Ribechini E, Greifenberg V, Sandwick S, & Lutz MB (2010) Subsets, expansion and activation of myeloid-derived suppressor cells. *Med Microbiol Immunol* 199(3):273-281.

28. Novitskiy SV*, et al.* (2011) TGF-beta receptor II loss promotes mammary carcinoma progression by Th17 dependent mechanisms. *Cancer Discov* 1(5):430-441.

29. Parker KH, Beury DW, & Ostrand-Rosenberg S (2015) Myeloid-Derived Suppressor Cells: Critical Cells Driving Immune Suppression in the Tumor Microenvironment. *Adv Cancer Res* 128:95-139.

30. Yang Z*, et al.* (2010) Mast cells mobilize myeloid-derived suppressor cells and Treg cells in tumor microenvironment via IL-17 pathway in murine hepatocarcinoma model. *PLoS One* 5(1):e8922.

31. Corzo CA*, et al.* (2010) HIF-1alpha regulates function and differentiation of myeloid-derived suppressor cells in the tumor microenvironment. *J Exp Med* 207(11):2439-2453.

32. Gabrilovich DI & Nagaraj S (2009) Myeloid-derived suppressor cells as regulators of the immune system. *Nat Rev Immunol* 9(3):162-174.

33. Hart KM, Byrne KT, Molloy MJ, Usherwood EM, & Berwin B (2011) IL-10 immunomodulation of myeloid cells regulates a murine model of ovarian cancer. *Front Immunol* 2:29.

34. Dugast AS*, et al.* (2008) Myeloid-derived suppressor cells accumulate in kidney allograft tolerance and specifically suppress effector T cell expansion. *J Immunol* 180(12):7898-7906.

35. Suh ED*, et al.* (1993) Splenectomy abrogates the induction of oral tolerance in experimental autoimmune uveoretinitis. *Curr Eye Res* 12(9):833-839.

36. Buettner M, Bornemann M, & Bode U (2013) Skin tolerance is supported by the spleen. *Scand J Immunol* 77(4):238-245.

37. Flugel A*, et al.* (2001) Migratory activity and functional changes of green fluorescent effector cells before and during experimental autoimmune encephalomyelitis. *Immunity* 14(5):547-560.

Figure legends

Figure 1. Increase in M-MDSCs and PMN-MDSCs during EDI. Shown are representative FACS plots from different organs from PBS-treated and MBP_{Ac1-9}(4Y)- treated TG4 animals, gated on single, viable $CD11b^+$ cells. Organs from PBS controls (**A**) or MBP_{Ac1-9}(4Y)-animals (**B**) were isolated and stained with a panel of antibodies and two subpopulations of MDSCs were identified by flow cytometry. Representative of three individual experiments. **C**) Shown is the frequency of PMN-MDSCs during EDI after the 3^{rd} and 5^{th} dose of MBP_{Ac1-9}(4Y) in various organs compared to control mice receiving one dose of PBS. The gating strategy excluded dead cells and doublets. Horizontal lines indicate mean. After checking for normality using the Shapiro-Wilk test the Kruskal-Wallis test followed by Dunn's multiple comparison test for data that were not normally distributed was used (* = $p \leq 0.05$, ** = $p \leq 0.01$, *** = $p \leq 0.001$, **** = $p \leq 0.0001$). In the spleen, ILNs, BLNs and lung each dot represents one individual mouse. In the liver in some cases cells from two animals were combined due to low cell numbers while in the CNS compartment each dot represents two individuals. N=6, from two independent experiments.

Figure 2. Phenotypic analysis of PMN-MDSCs after dose escalation immunotherapy. **A**) Representative flow cytometry plot of splenic PMN-MDSCs from MBP_{Ac1-9}(4Y)- (black line) and PBS control-treated (filled grey line) animals after gating on viable $CD11b^+$ $Ly6G^+$ cells and comparison of Galectin-9, PD-L1, CD40, CD80 and CD86 expression shown as histogram overlays. Dotted line indicates negative staining control. **B**) Bar graph shows mean + SEM. After checking for normality using the Shapiro-Wilk test either ANOVA

followed by Sidak's multiple comparison test was performed for normally distributed data or the Kruskal-Wallis test followed by Dunn's multiple comparison test for data that were not normally distributed (* = $p \leq 0.05$, ** = $p \leq 0.01$, *** = $p \leq 0.001$, **** = $p \leq 0.0001$). Data on the left of the vertical line had a normal distribution. In the spleen, ILNs, BLNs and lung each bar graph represents six individuals. In the liver in some cases cells from two animals were combined due to low cell numbers (n = 4) while in the CNS compartment each measurement contained cells from two animals. Kruskal-Wallis test followed by Dunn's multiple comparison test was applied to CD40, CD80 and CD86 data. N=6, from two independent experiments.

Figure 3. Splenic PMN-MDSCs suppress the proliferation of $CD4^+$ T cells in an antigen-specific manner. PMN-MDSCs were co-cultured for four days together with naïve (Tnaiv) and antigen-experienced T cells (Tag) labelled with cell proliferation dye at a ratio of 1:3 with their cognate peptide and $CD11c^+$ cells used as APCs. Gated on single, viable $CD4^+$ T cells. **A**) Proliferation of Tnaiv and Tag $CD4^+$ T cells after culture with or without PMN-MDSCs (n=5). Box shows 25th to 75th percentiles. The horizontal line is plotted at the median. Whiskers show Min to Max. Mean is shown as a '+'. B) Foxp3 expression in $CD4^+$ Tnaiv and $CD4^+$ Tag after culture with or without PMN-MDSC's (n=5). Box shows 25th to 75th percentiles. The horizontal line is plotted at the median. Whiskers show Min to Max. '+' indicates mean. After checking for normality using the Shapiro-Wilk test ANOVA followed by Sidak's multiple comparison test was performed for normally distributed data (* = $p \leq 0.05$, ** = $p \leq 0.01$, *** = $p \leq 0.001$, **** = $p \leq 0.0001$).

Figure 4. Splenic PMN-MDSCs suppress $CD4^+$ T cell proliferation induced by plate-bound anti-CD3 and anti-CD28 in a cell-contact dependent manner. Naïve (Tnaiv) (**A**) or antigen-experienced $CD4^+$ T cells (Tag) (**B**) labelled with cell proliferation dye, were cultured with PMN-MDSCs from either tolerised (n=6) or PBS-treated mice (n=3) on an anti-CD3+antiCD28-coated plate at a ratio of 1:1. **C**) Splenic, FACS-sorted PMN-MDSC from tolerised mice and $CD4^+$ Tag cells were cultured together at a ratio of 1:1 in on anti-CD3+anti-CD28-coated plate, separated by a membrane (n=3). Gated on single, viable $CD4^+$ T cells. Box shows 25th to 75th percentiles. The horizontal line is plotted at the median. Whiskers show Min to Max. '+' indicates mean. Kruskal-Wallis test followed by Dunn's multiple comparison test was performed for data that were not normally distributed (* = $p \leq 0.05$, ** = $p \leq 0.01$, *** = $p \leq 0.001$, **** = $p \leq 0.0001$).

Figure 5. Determination of the mechanism of PMN-MDSCs mediated $CD4^+$ T cell suppression *in vitro*. Splenic, FACS-sorted PMN-MDSC from tolerised mice and $CD4^+$ Tag cells were cultured together at a ratio of 1:1 on an anti-CD3+anti-CD28-coated plate. **A**) Antibodies to Galectin-9, PD-L1, CD40, CD80, CD86 and IL-10R (10 μg/ml) or **B**) chemical inhibitors of iNOS (L-NMMA) or arginase-1 (BEC) (both at 500 μM) were added for the duration of the culture (n = 3 each). Gated on single, viable $CD4^+$ T cells. Box shows 25^{th} to 75^{th} percentiles. The horizontal line is plotted at the median. Whiskers show Min to Max. '+' indicates mean. Kruskal-Wallis test followed by Dunn's multiple comparison test was performed (* = $p \leq 0.05$, ** = $p \leq 0.01$, *** = $p \leq 0.001$, **** = $p \leq 0.0001$).

Figure 6. Frequencies and phenotype of PMN-MDSCs in peripheral organs in diseased versus tolerised mice. Tg4 mice were treated with PBS or MBP_{Ac1-9}(4Y)-EDI before the induction of EAE. Animals were analysed at the peak of disease when mice treated with PBS showed complete hind limb paralysis (grade 3) and EDI-treated animals showed no sign of disease. **A**) Shown are single, viable $CD11b^+$ $Ly6G^+$ cells. Horizontal lines indicate mean. After checking for normality using the Shapiro-Wilk test the unpaired t test was performed for normally distributed data (* = $p \leq 0.05$, ** = $p \leq 0.01$, *** = $p \leq 0.001$, **** = $p \leq 0.0001$). Each dot represents one individual, n=7-11. Pooled data from three independent experiments. **B**) Single, viable PMN-MDSCs were analysed for the expression of CD40, CD80, Galectin-9 and PD-L1. Horizontal lines indicate mean. After checking for normality using the Shapiro-Wilk test either unpaired t test was performed for normally distributed data or the Mann-Whitney U test for data that were not normally distributed (* = $p \leq 0.05$, ** = $p \leq 0.01$, *** = $p \leq 0.001$, **** = $p \leq 0.0001$). Each dot represents one individual, n=7-11. Pooled data from three independent experiments. Unpaired t test was applied to CNS data. Unpaired t test was applied to Galectin-9 BLN data and PD-L1 data whereas the Mann-Whitney U test was applied to spleen Galectin-9 data.

Figure 7. Splenectomy impairs the increase in the number of PMN-MDSCs post EDI and prevents tolerance induction. Tg4 mice underwent either a sham operation or splenectomy 14 days before EDI to induce tolerance or PBS only as a control. Thereafter, ILNs, BLNs, lungs and liver were removed and analysed by flow cytometry (each dot represents an animal), gated on single,

viable cells. Horizontal lines in A and B indicate mean. After checking for normality using the Shapiro-Wilk test either ANOVA followed by Sidak's multiple comparison test was performed for normally distributed data or the Kruskal-Wallis test followed by Dunn's multiple comparison test for data that were not normally distributed (* = $p \leq 0.05$, ** = $p \leq 0.01$, *** = $p \leq 0.001$, **** = $p \leq 0.0001$). **A**) Percentage of $CD11b^+$ $Ly6G^+$ PMN-MDSCs in the ILN, BLN, lung and liver in splenectomised or sham-operated mice that have either been tolerised with MBP_{Ac1-9}(4Y) or received control treatment with PBS only. ANOVA followed by Sidak's multiple comparison test was applied to ILN (n=6-7, pooled data from 2 independent experiments) and BLN data (n=6-7, pooled data from 2 independent experiments). Kruskal-Wallis test followed by Dunn's multiple comparison test was applied to lung and liver data (n=3-4, one experiment). **B**) Absolute numbers of $CD11b^+$ $Ly6G^+$ PMN-MDSCs in the ILN, BLN, lung and liver in splenectomised or sham-operated mice that have either been tolerised with MBP_{Ac1-9}(4Y) or received control treatment with PBS only. ANOVA followed by Sidak's multiple comparison test was applied to ILN (n=6-7, pooled data from 2 independent experiments) and BLN data (n=6 -7, pooled data from two independent experiments). Kruskal-Wallis test followed by Dunn's multiple comparison test was applied to lung and liver data (n=3-4, one experiment). **C**) Tg4 mice underwent either sham operation or splenectomy 14 days before EDI to induce tolerance or were treated with PBS as a control. Subsequently, EAE was induced and animals were monitored daily for 20 days for signs of disease. Line graph shows disease scores over time (mean+SEM). Bar graph shows area under the curve (AUC, mean+SEM). One-way ANOVA with Tukey's

multiple comparison post hoc test $p \leq 0.05$, n=9-12 for each group, pooled data from three independent experiments, mean+SEM).

Figure 8. Signalling through the IL-10 receptor is required for PMN-MDSCs accumulation. Tg4IL-$10^{-/-}$ mice or wild-type Tg4 mice were either treated with PBS as a control or MBP_{Ac1-9}(4Y) according to the EDI protocol until the 3rd dose before isolating the spleen and lymph nodes to define quantity of PMN-MDSCs. Horizontal lines indicate mean. Each dot represents one individual, n=4-6, pooled data from three independent experiments. Kruskal-Wallis test followed by Dunn's multiple comparison test was performed for data that were not normally distributed (* = $p \leq 0.05$, ** = $p \leq 0.01$, *** = $p \leq 0.001$, **** = $p \leq 0.0001$). **A**) Percentages of $CD11b^+$ $Ly6G^+$ PMN-MDSCs in spleen and lymph nodes of PBS or MBP_{Ac1-9}(4Y)-treated wild-type Tg4 and Tg4IL-$10^{-/-}$ mice, gated on single, viable cells. **B**) Absolute numbers of $CD11b^+$ $Ly6G^+$ PMN-MDSCs in spleen and lymph nodes of PBS or MBP_{Ac1-9}(4Y)-treated wild-type Tg4 and Tg4IL-$10^{-/-}$ mice. Definition of the phenotype of PMN-MDSCs, gated on single, viable $CD11b^+$ $Ly6G^+$ PMN-MDSCs. N=4-6, pooled data from two to three independent experiments. Kruskal-Wallis test followed by Dunn's multiple comparison test was performed for data that were not normally distributed (* = $p \leq 0.05$, ** = $p \leq 0.01$, *** = $p \leq 0.001$, **** = $p \leq 0.0001$). Bar graph shows mean + SEM. **C**) CD80 expression on $CD11b^+$ $Ly6G^+$ PMN-MDSCs in spleen and lymph nodes of PBS or MBP_{Ac1-9}(4Y)-treated wild-type Tg4 and Tg4IL-$10^{-/-}$ mice. **D**) CD86 expression on $CD11b^+$ $Ly6G^+$ PMN-MDSCs in spleen and lymph nodes of PBS or MBP_{Ac1-9}(4Y)-treated wild-type Tg4 and Tg4IL-$10^{-/-}$ mice.

Figure 9. Adoptive transfer of PMN-MDSCs reduces $CD4^+$ T cell proliferation after antigen prime *ex vivo*. Tg4 mice received either a cell transfer of $1.5x10^6$ FACS sorted PMN-MDSC i.p. or no transfer three days before priming with MBP_{Ac1-9}(4K) peptide in CFA at the base of the tail. Ten days post-prime, spleen and ILNs were harvested and a ^{3}[H]-Thymidine assay set up. **A**) Proliferative response of whole cell isolates from the spleen and ILN, after restimulation *in vitro* with titrated doses of MBP_{Ac1-9}(4K) (n = 6 - 8, pooled data from two independent experiments). Line graph shows mean ± SEM. After checking for normality using the Shapiro-Wilk test the unpaired t test was performed for normally distributed data (* = $p \leq 0.05$, ** = $p \leq 0.01$, *** = $p \leq 0.001$, **** = $p \leq 0.0001$). **B**) Proliferative response of magnetically isolated $CD4^+$ T cells from the spleen and ILN, after restimulation *in vitro* with titrated doses of MBP_{Ac1-9}(4K) in the presence of irradiated APCs (n = 3). Mann-Whitney U test (* = $p \leq 0.05$, ** = $p \leq 0.01$, *** = $p \leq 0.001$, **** = $p \leq 0.0001$) **C**) ICCS of isolated single, viable $CD4^+$ T cells from spleen and lymph nodes. Each dot represents one individual (n=3). Horizontal lines indicate mean. (Mann-Whitney U test).

Figure 10. PMN-MDSCs limit the encephalogenicity of Th1 cells. Tg4 mice received an adoptive transfer of $5x10^6$ Th1 cells that were differentiated $^{in\ vitro}$ in the presence (PMN-MDSC-Th1) or absence of PMN-MDSCs (Th1) (n=5 per group). Line graph and bar graph show mean + SEM. Mann-Whitney U test was performed for comparison of mean EAE score of individual days. Unpaired t-test with Welch's correction was used for the comparison of AUCs. (* = $p \leq 0.05$, ** = $p \leq 0.01$, *** = $p \leq 0.001$, **** = $p \leq 0.0001$).

Table 1. PMN-MDSCs limit the encephalogenicity of Th1 cells. Tg4 mice received an adoptive transfer of $5x10^6$ Th1 cells that were differentiated in vitro in the presence (PMN-MDSC-Th1) or absence of PMN-MDSCs (n=5 per group). * Day of onset is the first day mice showed signs of EAE after cell transfer. † Incidence is the number of cases of EAE/number of mice immunized for each group.

treatment	**day of onset*** **mean ± SEM**	**incidence†**	**maximum score mean ± SEM**	**area under the curve mean ± SEM**
polarised under normal Th1 conditions				
Th1	6.8 ± 0.86	5/5	3 ± 0.54	32.6 ± 0.92
Th1 cells polarised under PMN-MDSCs influence				
PMN-MDSC-Th1	5.8 ± 0.36	5/5	2 ± 0	15.2 ± 0.27

A

CTRL

MBP_{Ac1-9}(4Y)

spleen | ILN | BLN | liver | lung | brain | spinal cord

Ly6 G

Ly6 C

B

% $CD11b^+$ $Ly6G^+$

spleen | ILN | BLN | liver | lung | brain | spinal cord

CTRL

MBP_{Ac-9} (4Y) 3rd dos.

MBP_{Ac1-9} (4Y) 5th dos.

C

cell number x (10^{-4})

spleen | ILN | BLN | liver | lung | brain | spinal cord

CTRL

MBP_{Ac-9} (4Y) 3rd dos.

MBP_{Ac1-9} (4Y) 5th dos.

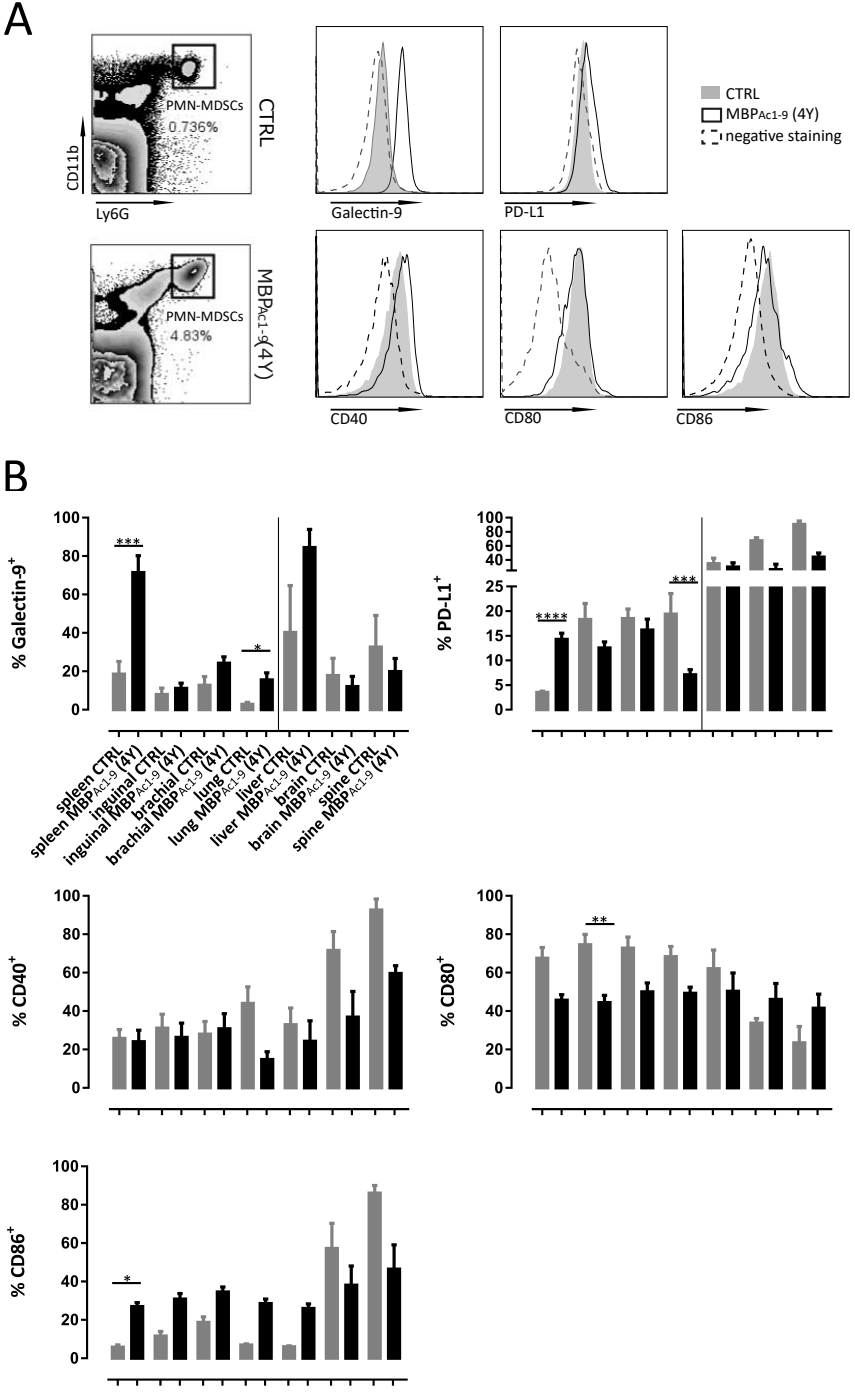
A
PMN-MDSCs
0.736%
CTRL
CD11b
Ly6G
Galectin-9
PD-L1
CTRL
MBPAc1-9 (4Y)
negative staining
PMN-MDSCs
4.83%
MBPAc1-9(4Y)
CD40
CD80
CD86
B
% Galectin-9+
% PD-L1+
% CD40+
% CD80+
% CD86+
spleen CTRL
spleen MBPAc1-9 (4Y)
inguinal CTRL
inguinal MBPAc1-9 (4Y)
brachial CTRL
brachial MBPAc1-9 (4Y)
lung CTRL
lung MBPAc1-9 (4Y)
liver CTRL
liver MBPAc1-9 (4Y)
brain CTRL
brain MBPAc1-9 (4Y)
spine CTRL
spine MBPAc1-9 (4Y)

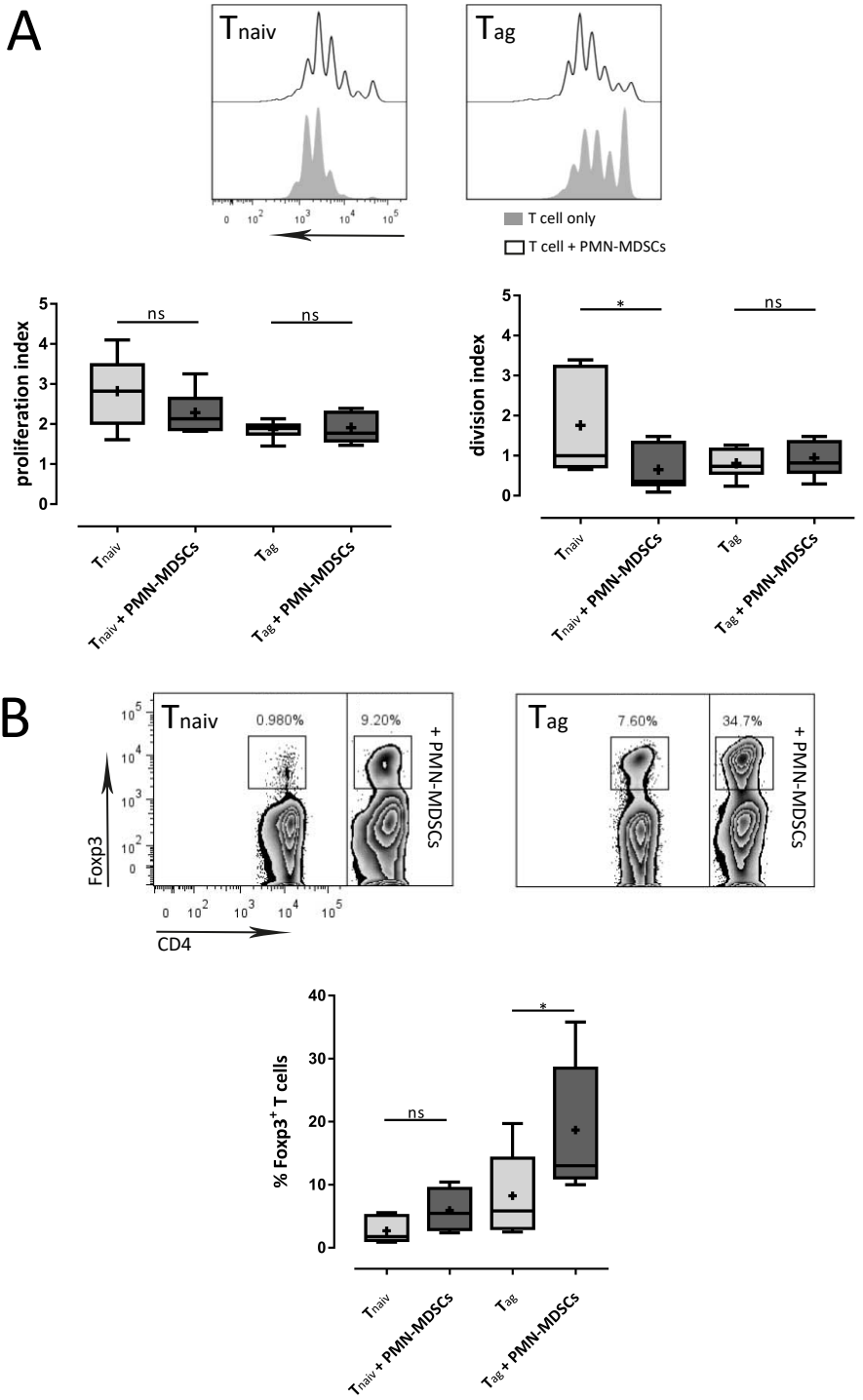
A
Tnaiv
Tag
T cell only
T cell + PMN-MDSCs
proliferation index
ns
ns
Tnaiv
Tnaiv + PMN-MDSCs
Tag
Tag + PMN-MDSCs
division index
*
ns
B
Tnaiv
0.980%
9.20%
+ PMN-MDSCs
Foxp3
CD4
Tag
7.60%
34.7%
% Foxp3+ T cells
ns
*

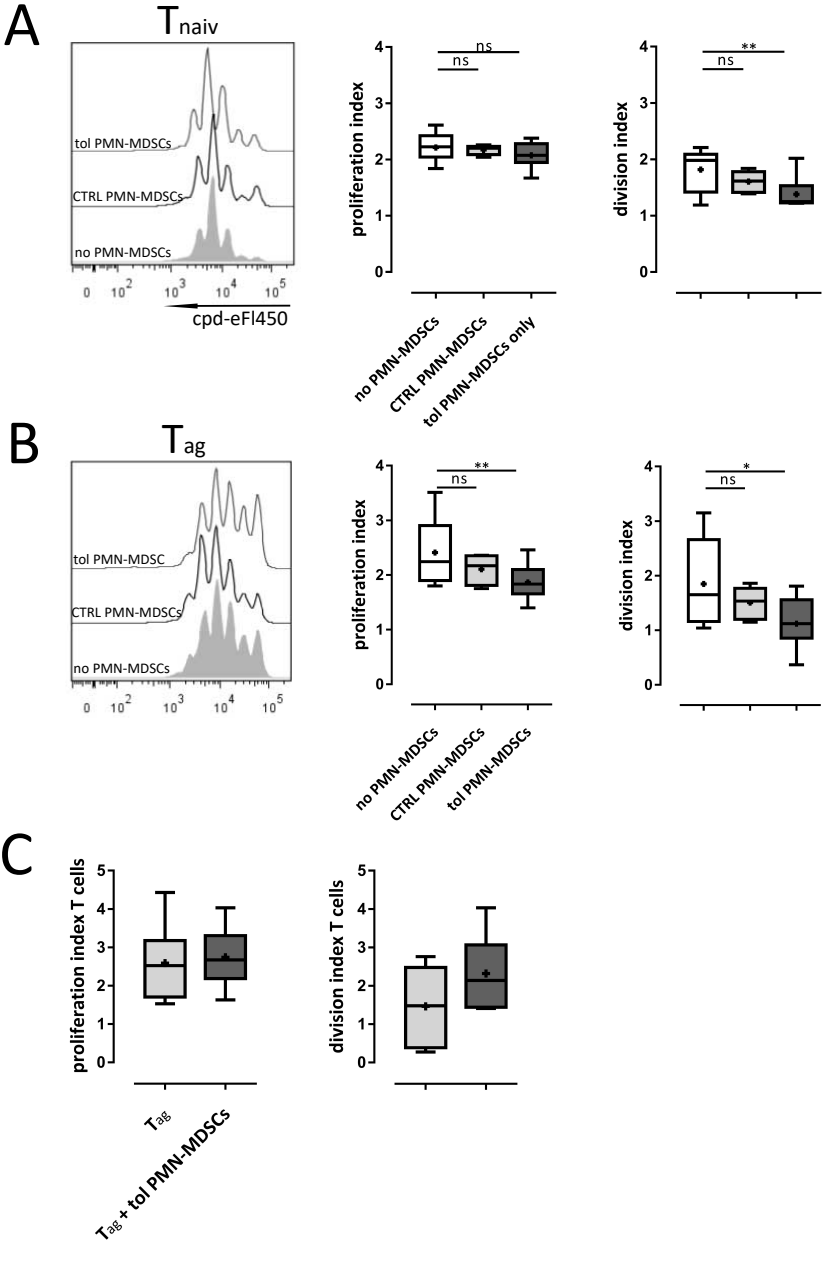
A
Tnaiv
tol PMN-MDSCs
CTRL PMN-MDSCs
no PMN-MDSCs
cpd-eFl450
proliferation index
division index
ns
**
no PMN-MDSCs
CTRL PMN-MDSCs
tol PMN-MDSCs only
B
Tag
tol PMN-MDSC
CTRL PMN-MDSCs
no PMN-MDSCs
*
C
proliferation index T cells
division index T cells
Tag
Tag + tol PMN-MDSCs

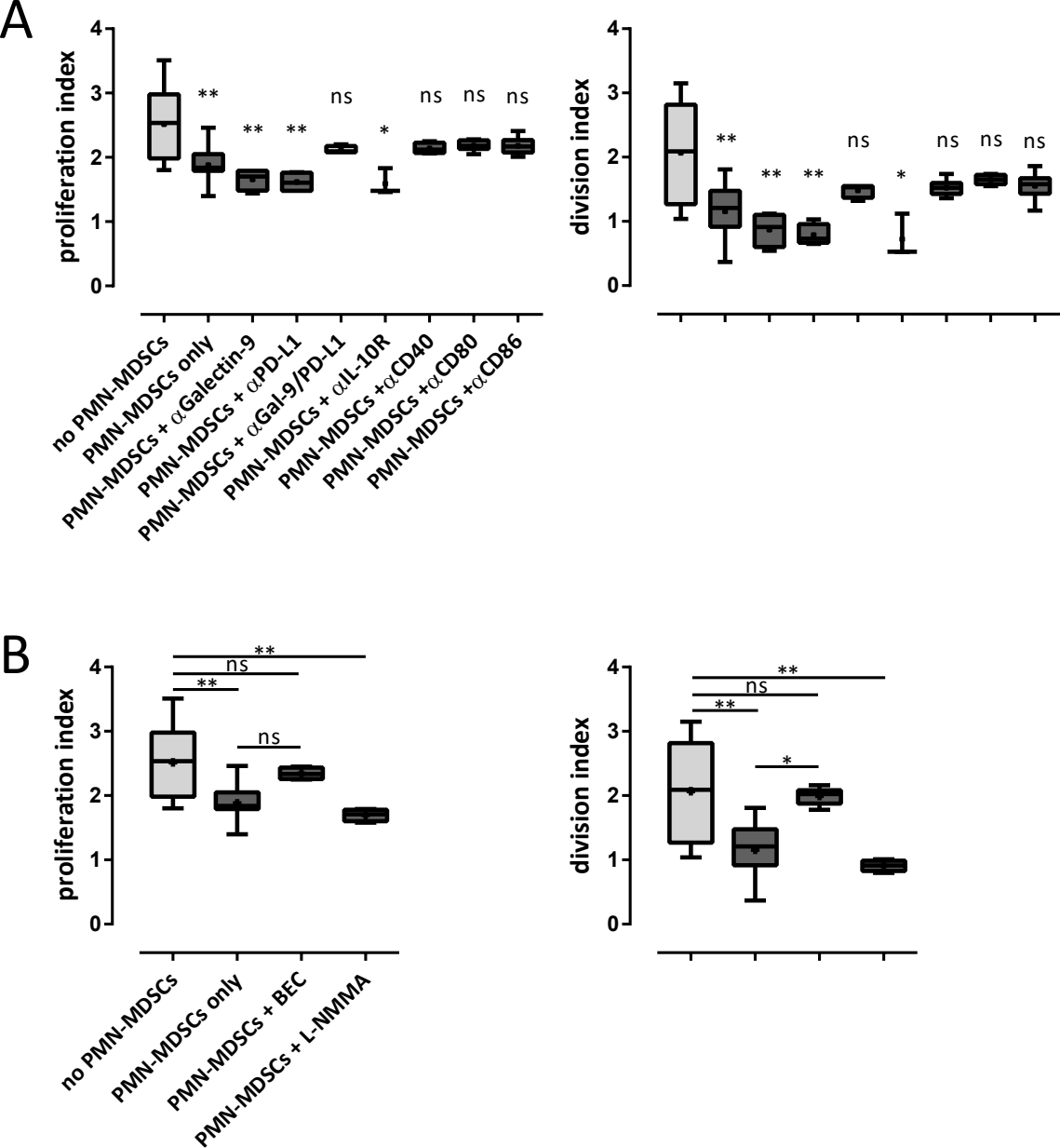
A
proliferation index
division index
0
1
2
3
4
**
**
**
ns
*
ns
ns
ns
no PMN-MDSCs
PMN-MDSCs only
PMN-MDSCs + αGalectin-9
PMN-MDSCs + αPD-L1
PMN-MDSCs + αGal-9/PD-L1
PMN-MDSCs + αIL-10R
PMN-MDSCs +αCD40
PMN-MDSCs +αCD80
PMN-MDSCs +αCD86
B
proliferation index
division index
**
ns
**
ns
*
no PMN-MDSCs
PMN-MDSCs only
PMN-MDSCs + BEC
PMN-MDSCs + L-NMMA

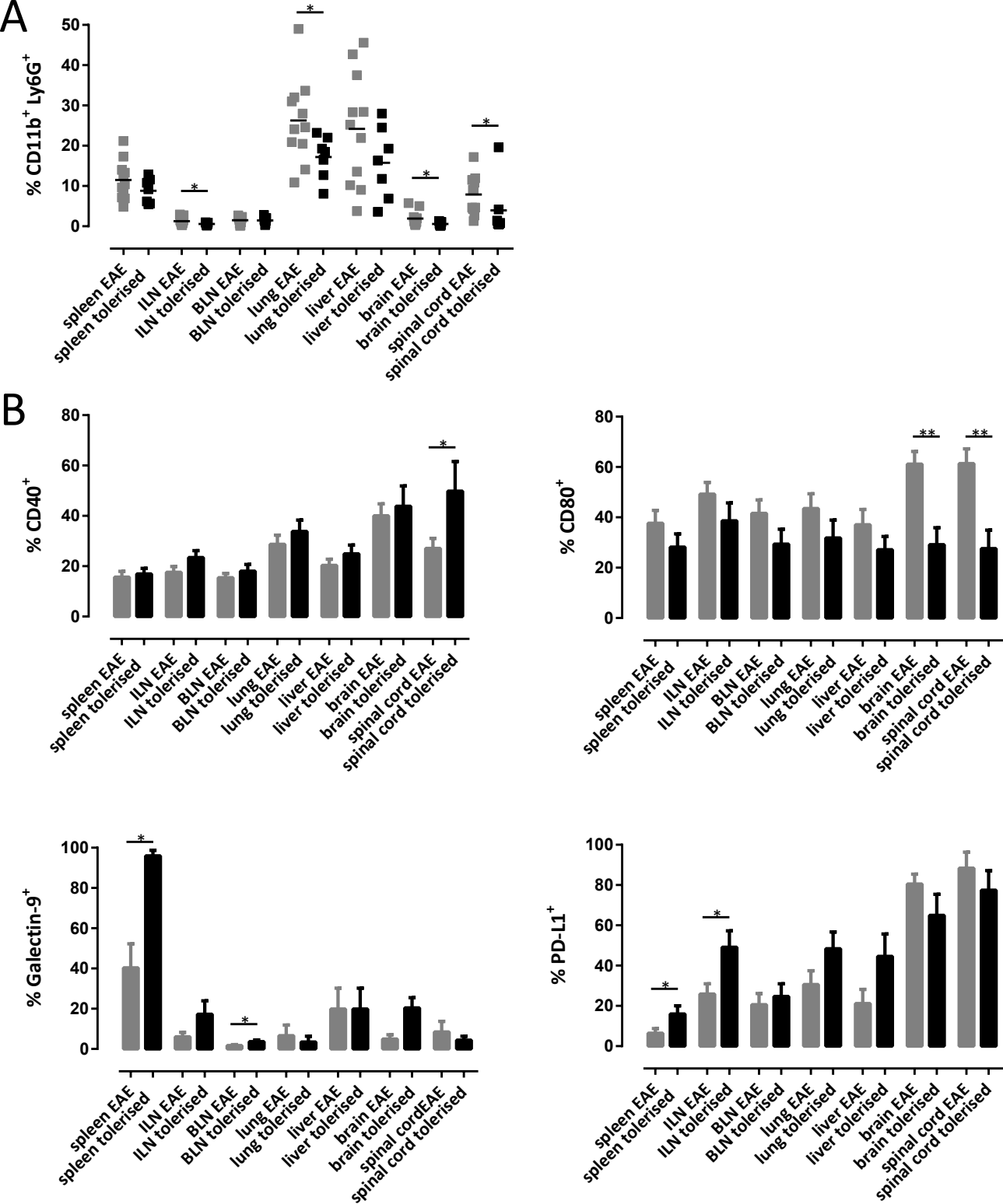
A
% CD11b+ Ly6G+
B
% CD40+
% CD80+
% Galectin-9+
% PD-L1+
spleen EAE
spleen tolerised
ILN EAE
ILN tolerised
BLN EAE
BLN tolerised
lung EAE
lung tolerised
liver EAE
liver tolerised
brain EAE
brain tolerised
spinal cord EAE
spinal cord tolerised

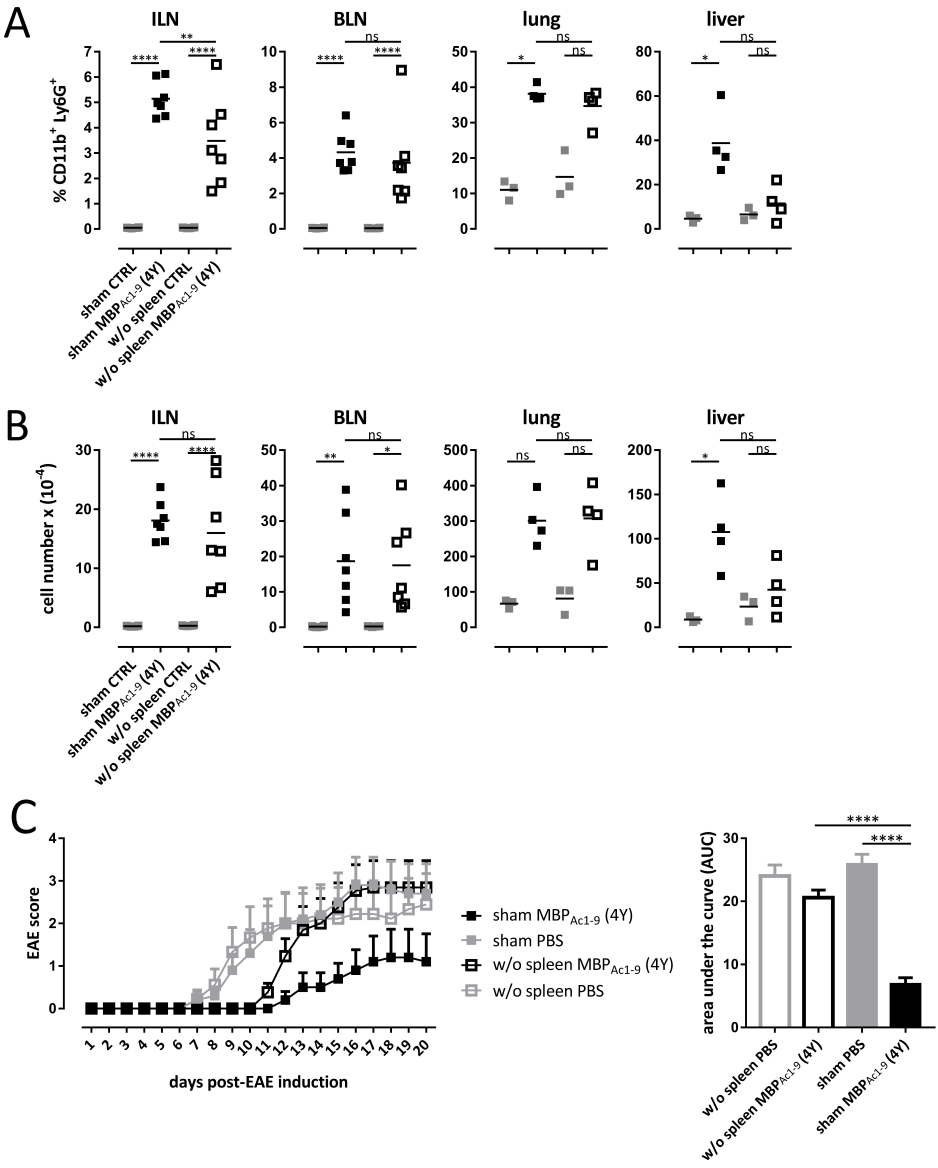
A
ILN
BLN
lung
liver
% CD11b+ Ly6G+
sham CTRL
sham MBPAc1-9 (4Y)
w/o spleen CTRL
w/o spleen MBPAc1-9 (4Y)
B
cell number x (10-4)
C
EAE score
days post-EAE induction
sham MBPAc1-9 (4Y)
sham PBS
w/o spleen MBPAc1-9 (4Y)
w/o spleen PBS
area under the curve (AUC)

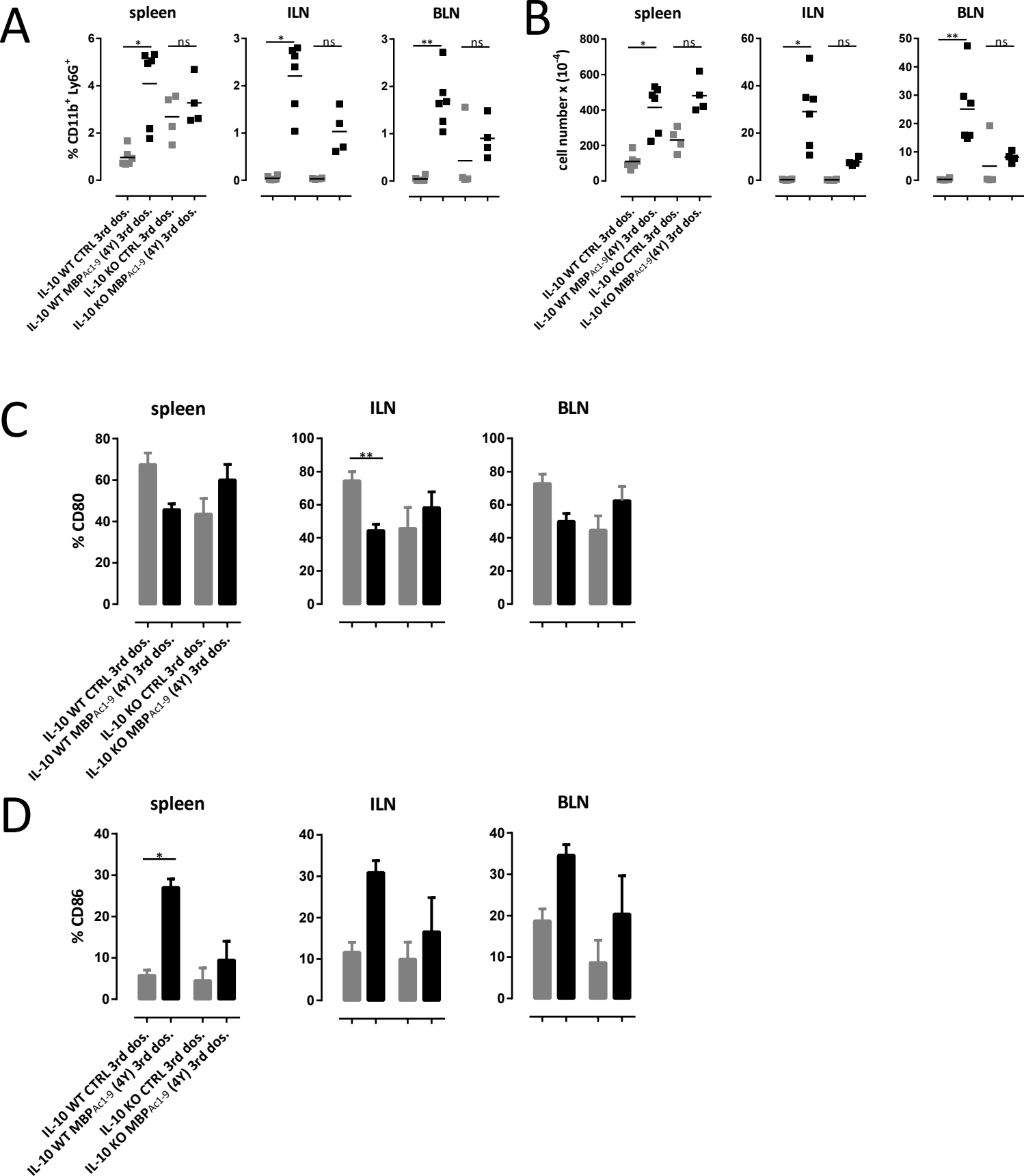
A
spleen
ILN
BLN
% CD11b+ Ly6G+
*
ns
**
IL-10 WT CTRL 3rd dos.
IL-10 WT MBPAc1-9 (4Y) 3rd dos.
IL-10 KO CTRL 3rd dos.
IL-10 KO MBPAc1-9 (4Y) 3rd dos.
B
spleen
ILN
BLN
cell number x (10-4)
*
ns
**
IL-10 WT CTRL 3rd dos.
IL-10 WT MBPAc1-9(4Y) 3rd dos.
IL-10 KO CTRL 3rd dos.
IL-10 KO MBPAc1-9(4Y) 3rd dos.
C
spleen
ILN
BLN
% CD80
**
IL-10 WT CTRL 3rd dos.
IL-10 WT MBPAc1-9 (4Y) 3rd dos.
IL-10 KO CTRL 3rd dos.
IL-10 KO MBPAc1-9 (4Y) 3rd dos.
D
spleen
ILN
BLN
% CD86
*
IL-10 WT CTRL 3rd dos.
IL-10 WT MBPAc1-9 (4Y) 3rd dos.
IL-10 KO CTRL 3rd dos.
IL-10 KO MBPAc1-9 (4Y) 3rd dos.

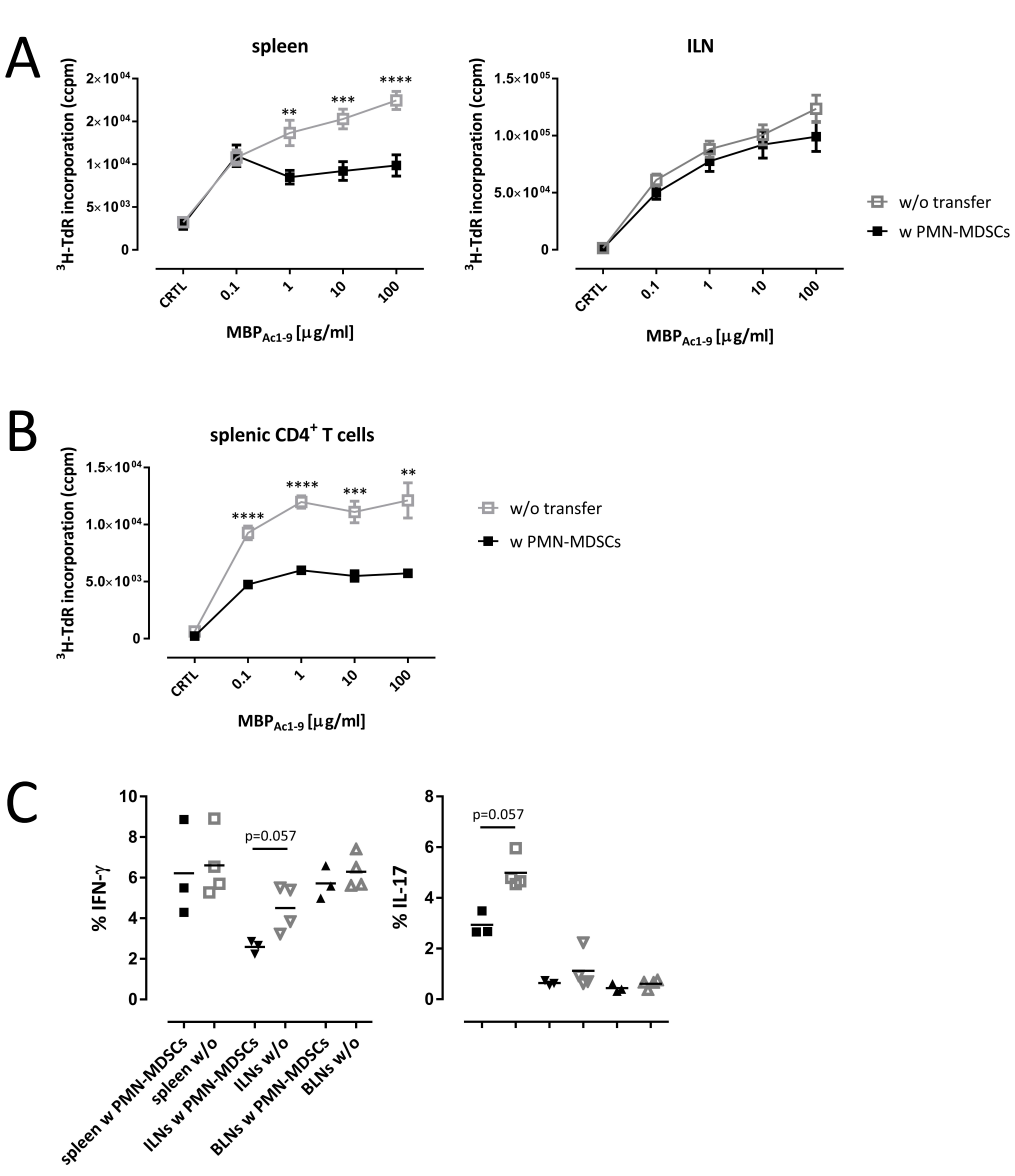
A
spleen
ILN
^{3}H-TdR incorporation (ccpm)
2×10^{04}
2×10^{04}
1×10^{04}
5×10^{03}
0
1.5×10^{05}
1.0×10^{05}
5.0×10^{04}
**
***
****
CRTL
0.1
1
10
100
MBP$_{Ac1-9}$ [μg/ml]
w/o transfer
w PMN-MDSCs
B
splenic CD4$^+$ T cells
1.5×10^{04}
1.0×10^{04}
5.0×10^{03}
****
****
***
**
C
% IFN-γ
% IL-17
p=0.057
p=0.057
spleen w PMN-MDSCs
spleen w/o
ILNs w PMN-MDSCs
ILNs w/o
BLNs w PMN-MDSCs
BLNs w/o

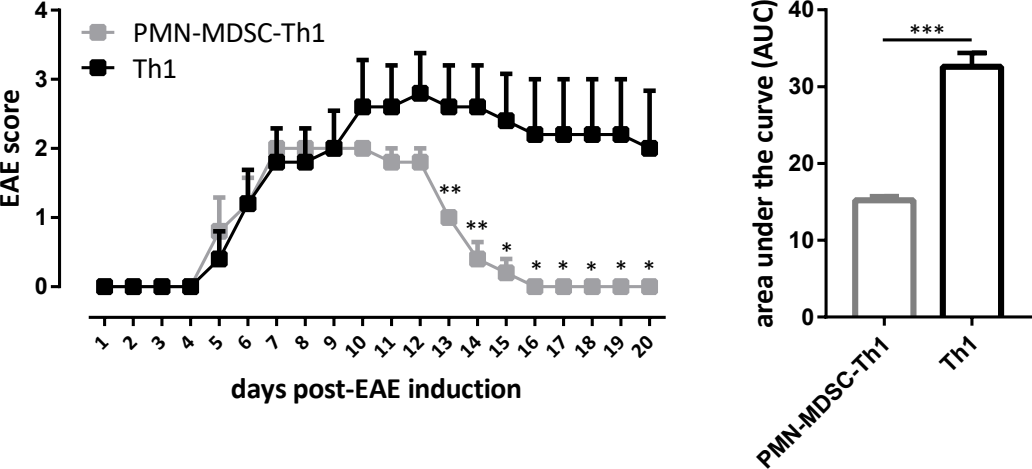
PMN-MDSC-Th1
Th1
EAE score
4
3
2
1
0
**
**
*
* * * * *
1 2 3 4 5 6 7 8 9 10 11 12 13 14 15 16 17 18 19 20
days post-EAE induction
area under the curve (AUC)
40
30
20
10
0
***
PMN-MDSC-Th1
Th1